Hammering Mechanism for HP3 Experiment (InSight)

Jerzy Grygorczuk[1,2], Łukasz Wiśniewski[1,2], Bartosz Kędziora[1,2], Maciej Borys[1,2], Rafał Przybyła[1,2], Tomasz Kuciński[1,2], Maciej Ossowski[3], Wojciech Konior[1,2], Olaf Krömer[4], Tilman Spohn[5], Marta Tokarz[2] and Mateusz Białek[1,2]

Abstract

This paper provides a description of the specific design features and nuances of the Hammering Mechanism, a drive unit for the HP3 mole-type penetrator for NASA's InSight mission. State of the art for this type of mechanism and an overall system overview are provided. Particular attention is focused on key components of the system that make it an effective mechanism. The main design changes introduced to the mechanism are related to three main domains: mechanism architecture and principles, increase of efficiency and simplification of the design, and functionality. A few critical lessons learnt are also described.

Introduction

The following paper discusses the development of the Hammering Mechanism (HM) for the HP3 mole-type penetrator – the drive unit of DLR's heat probe instrument for NASA's InSight mission. The Hammering Mechanism is a drive system of the HP3 penetrator whose purpose is to transport thermal sensors more than the required three meters below Martian surface (5 meters being the desired depth) [4]. The original concept of the mole-type penetrator mechanism was provided by Gromov et al. in [1] and then evolved through the PLUTO instrument for the Beagle2 mission [2], the proposal for an ExoMars instrument [3], to implementation in the InSight mission [4]. The most recent development of the Hammering Mechanism was done by Astronika and the Space Research Centre of the Polish Academy of Sciences (CBK), under contract and in close cooperation with DLR. Even though the concept remains the same, the final design, as implemented by Astronika for the purpose of this mission, significantly improved the system's performance with respect to the previous ones.

The article begins with a general introduction of the penetrator's design and their known solutions (state of the art). The specific system architecture of the HP3 Hammering Mechanism is provided in the System Overview section. The core of the paper comprises particular design features that made the mechanism more effective and improved its performance. This includes spring distribution, cam optimization, bearing description, dedicated roller design, multiple locking/unlocking launch lock system, and the mechanism's lubrication and coatings principles that significantly simplified the mechanism and increased its performance with respect to previous versions. Provided at the end are three lessons learned, which concern problems with cracking of tungsten alloys, removal of a spring clutch and the improper harness tensioning that may lead to a decrease in the penetrator's performance if not properly done.

State of the Art

The Hammering Mechanism (HM) mentioned in this text is part of a bigger system of a mole-type penetrator HP3 and its Support Structure onboard the InSight lander (Figure 1). A mole-type penetrator, in general, is an assembly that consists of three main assemblies: Hammer (HA), Suppressor Mass (SM), and Outer

[1] ASTRONIKA Sp. z o.o., Warsaw, Poland

[2] Space Research Centre of the Polish Academy of Sciences, Warsaw, Poland

[3] Warsaw University of Technology, Warsaw, Poland

[4] German Aerospace Center (DLR), Institute of Space Systems, Bremen, Germany

[5] German Aerospace Center (DLR), Institute of Planetary Research, Berlin, Germany

Casing with the Payload. The original idea of the system was provided in [1] and in principle, the Hammer is pulled up on its Cam by the rotational movement of a motor axis with a roller which periodically loads the Drive Springs located between the Hammer and the Suppressor Mass. After release from the Cam, the Hammer accelerates downwards eventually hitting the Outer Casing and causing its penetration, whereas the Suppressor Mass travels upwards and its movement is compensated by a Brake Spring and Wire Helix in its rear part.

a) 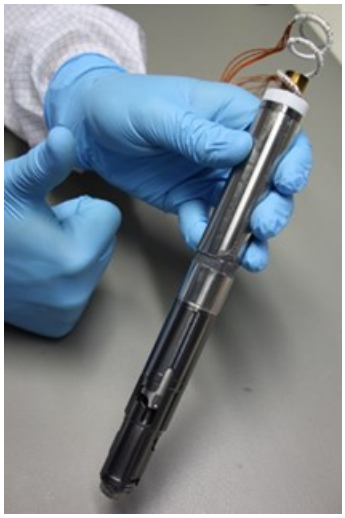 b) 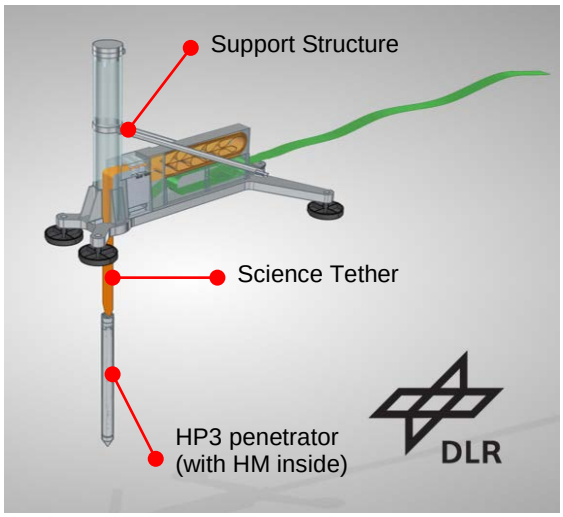

Figure 1. a) HP3 Hammering Mechanism (FS), b) HP3 overall system (credits: DLR)

The energy distributed between the Suppressor Mass and the Hammer depends on the mass ratio between those two assemblies. In some sense, the penetrator behaves like a mechanical diode, with high penetrating force provided by the Hammer's impact on the Outer Casing and a small pulling up reaction force. The Suppressor Mass travels up adequately and its kinetic energy is compensated by gravitational potential and compression of a Brake Spring located between the Suppressor Mass and the Outer Casing. The reaction force of the Brake Spring should be less than the holding forces of the Support Structure that guides the penetrator at the beginning of movement, and later the friction force between the Outer Casing and the regolith. The detailed sequence of operation was provided in [5] for HP3 and also in [6] and [7] for CBK's KRET developments.

The HP3 penetrator uses a cam mechanism to perform the strokes, which has clear advantages like: the simplicity of control (just powering the motor in one direction), straightforward locking and unlocking of the system using the rotating movement of the motor, and space heritage through the development of PLUTO for the Beagle 2 mission [1, 2, 3]. The disadvantage is a relatively short compression of the drive spring (and hence stroke energy), which is limited by the height of the cam. Inspired by PLUTO's design, NASA engineers also developed a spring-loaded mole-type penetrator [8].

Contrary to DLR's solution, CBK developed another mechanical penetrator – KRET, which also accumulates stroke energy in a spring, but this solution used a special latch grip which allowed the motor to perform multiple rotations before the hammer was latched. As a result higher compression values could be achieved as well as higher stroke energies (2.2 J in KRET 1 and 3.5 J in KRET 2), see [6]. In this solution the motor's current was monitored and the direction of movement of the motor interchanged accordingly.

Aside from the mechanical solutions, electromagnetic ones are known and utilized, for instance the space flown (TRL 9) MUPUS device for ESA's Rosetta mission [9]. This type of penetrator has the energy stored in a capacitor and released through an electromagnetic coil with a hammer accelerated as a moving core of the electromagnet. Based on this design further developments were provided, such as the CHOMIK device for the Phobos-Grunt mission [10], and the prototype of a High Energy and Efficiency Penetrator [11]. The disadvantage of such a solution is that it requires a capacitor that should be close to the drive coil

and as a consequence occupies a lot of volume, limiting the depth of penetration to the length of the penetrating rod (the drive unit is kept above the surface). The remaining qualities are just advantages like simplicity and reliability of the system as well as the possibility to apply different energy levels. There exists a prototype of an electromagnetic mole-type penetrator, where the capacitor was removed outside the outer casing and a stock of 5 electromagnets was used; it is the recently developed EMOLE within ESA PECS project [12].

System Overview

The Hammering Mechanism, as specifically mentioned in this paper, is located inside the Outer Casing and consists of the Hammer and the Suppressor Mass assemblies, together with Drive Springs, a Brake Spring and a Wire Helix (see Figure 2). From the point of view of integration, the HM is divided into: Hammer Lock Assembly (HLA), Axis Bearing Assembly, and Motor Assembly (MA). HM is guided against Outer Casing with a so-called Tongue Assembly, which is also important for the launch lock feature of the device. The actual details and components of the design are shown in Figure 2.

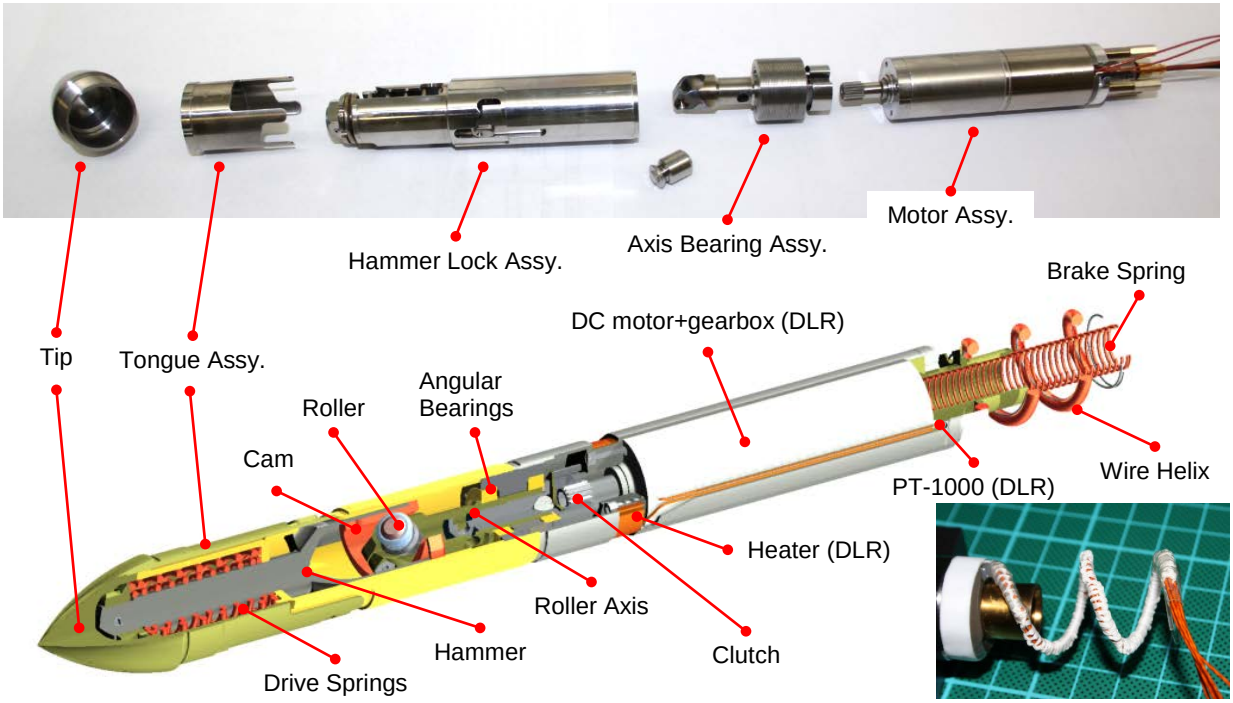

Figure 2. Components of HM. top: pre-PFM parts, bottom right corner: Wire Helix

The HLA consists specifically of the Hammer mounted with the Cam located inside the Hammer Housing. Two drive springs (inner and outer) are used with opposed coil turns and are located freely inside the Hammer Housing. They are protected against falling off by a Hammer Nut (screwed and pinned at the tip of the Hammer). The HLA is fixed with the MA through the Bearing Housing that is a part of the Axis Bearing Assembly. The HLA and the MA are counter torqued against each other on the Bearing Housing's thread. The pair of angular bearings located in the Bearing Housing provide axial rotation for the Roller Axis. The Axis is coupled with a gear shaft through a Clutch Element, which provides 40° of angular deadband in the movement of the axis. This angle is important for the phase of operation when the Roller (mounted at the end of the Roller Axis) falls off the Cam's edge and rotates freely the Axis with respect to the Cam to allow for the unconstrained movement of the Hammer.

As a drive unit, a customized Maxon DC Motor Unit DCX22 with Planetary Gearhead GP 22 HP is used, which was installed inside the Motor Housing by screws and using 3M Scotch Weld Epoxy Adhesive 2216 B/A Gray as a filler. Near the front part of the gear box and outside of the Motor Housing, a heater was

mounted to provide temperature control of the Motor Unit. A single PT-1000 sensor, used to monitor the temperature, was mounted in the back plate of the Motor Unit and covered with a Spring Support part. The DC motor, heater and PT-1000 were components for which DLR was responsible.

The MA is finished with the already mentioned Spring Support, which guides all 6 cables, protects their solder points (covered completely with 3M Scotch Weld Epoxy Adhesive 2216 B/A Gray), and provides space for beginning of a Wire Helix formation. The Wire Helix is a bundle of cables partially thermally formed and distributed along a Wire Guide (a gentle compressive spring) wrapped together into a continuous splice using lancing tape. The Brake Spring is a relatively narrow compression spring located inside the Spring Support (Wire Helix remains in parallel to it - outside the Spring Support). For this reason it is prone to buckle, but the Spring Support is long enough to provide constant guiding of the Brake Spring together with the corresponding Inner Guide on the side of the Payload Cage. The actual description of the rest of the HP3 mole penetrator system including Payload cage and Outer casing can be found in [5].

Worth mentioning is that in some sense each penetrator, including the HP3 instrument, may become a self-destructive device if is not designed correctly. Consequently, each joint and connection between parts have to be selected carefully, and, given the very limited volume for the mechanism, most of them have to be connected permanently. For instance, Araldite AV138/HV998 adhesive was used on threads to protect them from unscrewing, tight fit dowels used to connect Cam with the Hammer, press-fits and riveting of the Roller parts and welding in the Tongue Assembly elements. In most cases, disassembly of such connections is not possible without partial destruction of the mechanism.

Design Improvements and Significant Technological Features

The actual cooperation with DLR in the field of the Hammering Mechanism redesign and development began in late 2013. As a result of this cooperation, the final hardware was significantly improved in comparison to the previous versions [1, 2, 3]. Having an easy access to the in-house workshop and vast heritage in penetrators' design, the Space Research Centre PAS and Astronika, in cooperation with Warsaw University of Technology that provided tribological surfaces, was capable of rapid changes in the design and actually developed a new Hammering Mechanism for the HP3 mole instrument. The actual concept change was provided in November 2013, design freeze in December 2013 and successfully working pre-PFM model operating in February 2014. Six models were developed in total in years 2013-2015: pre-PFM, HM-1, HM-2, HM-3 (Life Test Unit), HM-4 (FM) and HM-5 (FS). The final design consists of 38 individual parts and components (82 total parts). The main design changes are described below and are related to three main domains: mechanism architecture and principles (rearrangement of subassemblies' layout and order), increase of efficiency and simplification of the design (improvement of tribological properties and bearings implementation), and functionality (launch lock redesign).

No preload on the drive springs

In the previous design the drive spring was preloaded, which theoretically could result in better utilization of the spring's characteristics. In fact, it is particularly important to sustain a free movement of the Hammer and the Suppressor-Mass in this type of mechanism, even at the expense of preload benefits. For this reason the preload option was removed and replaced with a free movement of all assemblies. This simplifies the behavior of the mechanism and consequently travel phases of each assembly and its impact moments can be clearly distinguished. The preloaded spring constrained the previous design to have the drive spring located between the rear part of the Hammer and front of the Motor Assembly. This caused the improper load distribution on the Hammer; namely it was pushed from behind instead of being pulled from the front, as it eventually was solved. Application of the pulling force in front of the Hammer (precisely on the Hammer Nut) naturally stabilizes the Hammer movement in the Hammer Housing and cancel all clamping possibilities or friction losses. The actual loading sequence is shown in Figure 3.

a) b) 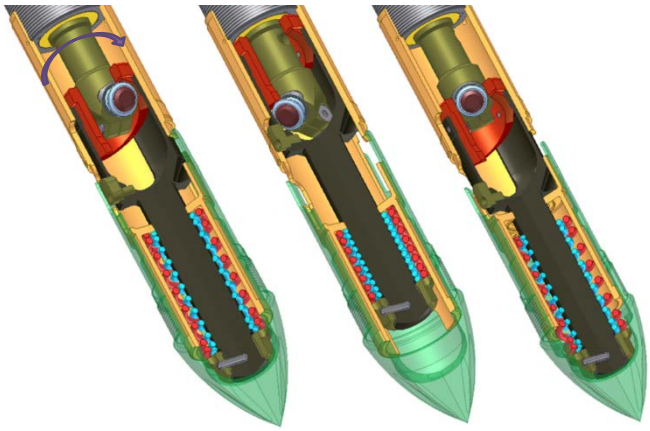

Figure 3. a) Hammer Lock Assembly, b) Cam loading Drive Springs compression sequence inside the Hammer Housing (Cam-Roller engagement, disengagement, travel of Hammer)

Cam optimization

Resignation from the spring preload, prompted the requirement to use higher cam inclination to provide higher spring compression and increase accumulated energy. A new approach to the cam design was undertaken with the following assumptions: the torque characteristics should be constant for most of the cycle time, the overall angular width of the cam is 280°, maximum reasonable angle at which the roller can roll in is 30° and allowable cam height is 15 mm (in contrast to the previous 7.8 mm). Eventually, the Cam starts with 30° angle inclination and continues until the plateau of constant torque is reached (which is at about 78° of Cam angle, this corresponds to 0.2 Nm of constant torque), then the inclination of the cam smoothly decreases to keep the resulting torque at the same level together with the increasing force of the drive springs. The actual cam profile and expected torque characteristics together with corresponding equations are shown in Figure 4 and Figure 5 (friction losses are assumed to be negligible). The symbols' meanings are: φ – angle of the Cam; φ_0 – angle of the Cam at which the inclination starts to change from 30°; $h(\varphi)$ – height of the Cam; $T(\varphi)$ – expected torque on the gear shaft; R – radius from the rotational axis to the working point of the Roller at the Cam; k – stiffness of the Drive Springs. Additional advantage of higher cam is that when Roller disengages from the Cam losses are expected, and partially the actual few millimeters of the height of the cam is not 100% effective. Hence, it is much better to have higher cam since this transition phase (between rolling and falling) has twice smaller relative contribution to the disturbance of the movement of the Hammer. It has also much more travel distance to accelerate and provide effective impact on the Outer Casing.

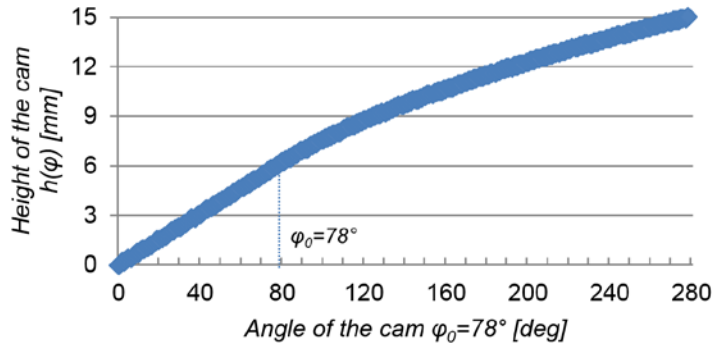

$$h(\varphi)=\begin{cases}\frac{\sqrt{3}}{3}R\varphi, & \text{for } \varphi\in[0°,\varphi_0]\\ R\sqrt{\frac{\varphi_0(2\varphi-\varphi_0)}{3}}, & \text{for } \varphi\in(\varphi_0,280°]\end{cases}$$

Figure 4. Theoretical shape of the Cam (symbols for equation described in the text)

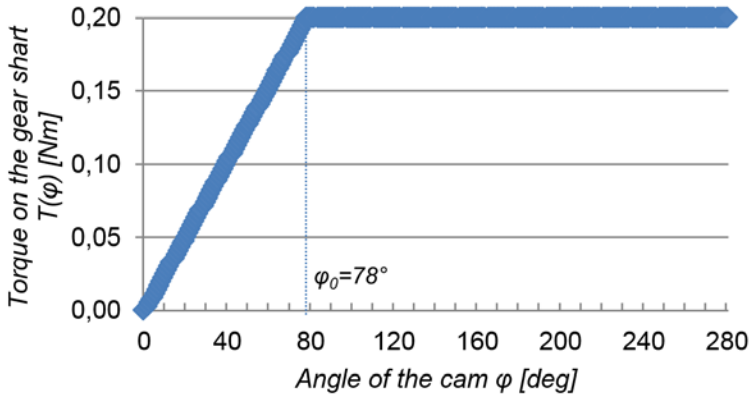

$$T(\varphi)=\begin{cases}\frac{1}{3}kR^2\varphi, & \text{for } \varphi\in[0°,\varphi_0]\\ \frac{1}{3}kR^2\varphi_0, & \text{for } \varphi\in(\varphi_0,280°]\end{cases}$$

Figure 5. Theoretical torque on the gear shaft and (symbols for equation described in the text)

Mass distribution and energy optimization

The proper mass ratio of the Outer Casing, Hammer and Suppressor Mass plays an important role in the system's efficiency and performance. It is particularly important to have the highest possible mass of the Suppressor Mass assembly and the lowest mass of the Hammer Assembly. This will result in high energetic stroke of the Hammer and low kinetic energy of the SM assembly to be compensated by the Brake Spring and the Wire Helix. At the same time, the mass of the Hammer Assembly should be balanced with the mass of the Outer Casing to achieve the best possible energy transfer between those assemblies. High density materials were used to accomplish this in the limited volume of the mechanism; in particular tungsten alloys were used for the Hammer (Wolfmet HE3925 alloy) and the Motor Housing (Wolfmet HE395). HE3925 remains more ductile, which was particularly important for the Hammer – the part that experiences the highest loads (over 10000g). Incidents of cracking were encountered in the scope of the project (described in the lessons learnt section), nevertheless the Hammering Mechanism together with the selected materials proved its durability in thousands of strokes performed (qualification level was 45000 strokes). The achieved mass ratios also allowed for the use of more energetic drive springs (c.a. 0.7 J), which is an important factor to sustain effectiveness or even allow for penetration of the mole in the regolith. In the final design, the achieved masses of the Hammer and Suppressor Mass assemblies are 0.11 kg and 0.46 kg correspondingly, so the actual Hammer kinetic energy is about 0.57 J and for the Suppressor Mass is 0.14 J.

Lubrication plan

All of the sliding bushings were replaced either with ball bearings (for all rolling movements) or advanced tribological surfaces that were provided by Warsaw University of Technology and Lodz University of Technology. This led to the vast simplification of the mechanism's design and also increase in its efficiency. Different coatings and surface treatments were used wherever applicable: lead (PVD), MoS_2 (PVD), TiN. The general rules were to: 1) use MoS_2 on all sliding surfaces (it was also used on tungsten alloy for the first time), 2) lead on rolling or stroke surfaces and also springs, 3) and TiN on all titanium surfaces. All surfaces were hardened (nitrided) before the deposition of coatings, with the exception of Tungsten alloys, which reveal relatively larger hardness on their own (24-26 HRC). The actual main materials and tribological coatings are shown in Figure 6.

The applied surface modification processes increased wear resistance of the used steel, titanium and tungsten parts of the HP3 device. Applying MoS_2 magnetron sputtered coating significantly reduced wear rates and friction coefficient of these materials. In case of titanium alloy (Ti6Al4V), additional plasma nitriding process was necessary in order to improve the lifetime of MoS_2 coating. Additional tests using „ball on disc" tribometer with Al_2O_3 ball were performed to prove the rightness of MoS_2 application on Tungsten (HE 395) and titanium alloy (tests in air). As it can be seen in Figure 7 the coefficient of friction for tungsten alloy has significantly reduced and stabilized after MoS_2 deposition (from 0.5-0.7 to below 0.1). For the case of titanium alloy, the tests revealed that the use of nitride titanium surface as a base surface for MoS_2 deposition can increase the wear resistance of the coating over two times (the test ended after 1100 m).

Additional tests for this type of tribological pair can be found in [13]. Figure 8 shows wear traces of the tested samples clearly showing higher wear resistance for nitrided titanium and tungsten with MoS_2 sputtered.

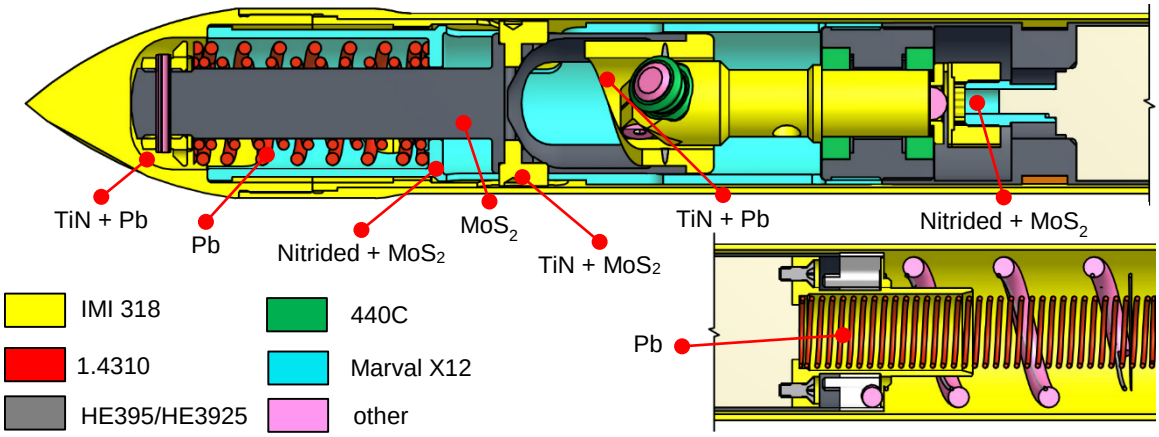

Figure 6. Materials and coatings of the Hammering Mechanism

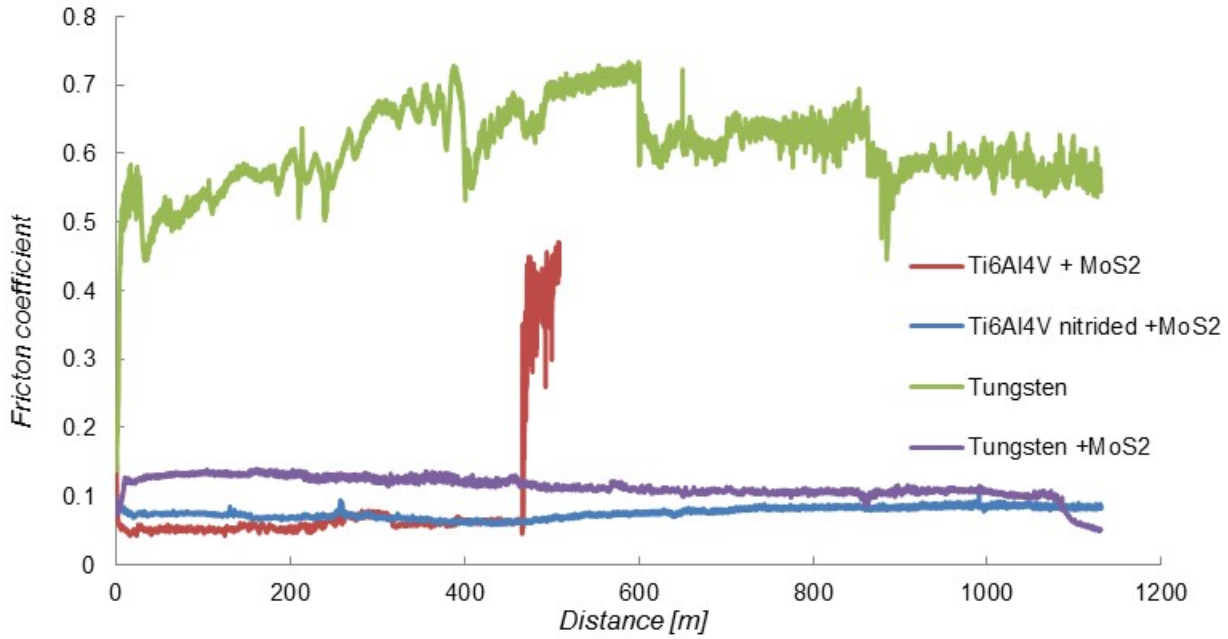

Figure 7. Friction coefficient changes as a function of friction distance of used materials after different surface treatments ("ball on disc" test against Al_2O_3 ball under 10-N load) in air

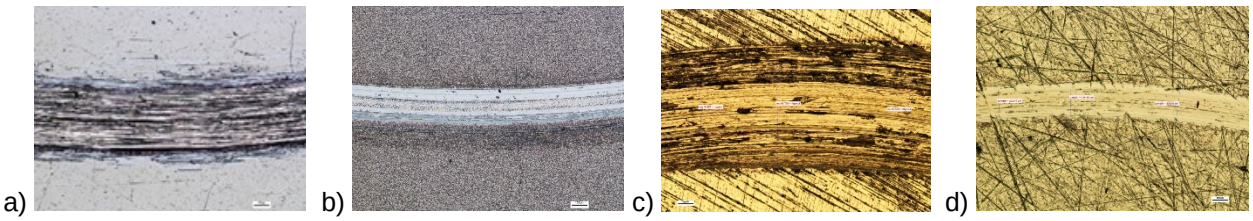

Figure 8. Wear traces of Ti6Al4V (a), nitrided Ti6Al4V (b) and tungsten alloy (d) coated by MoS_2 in comparison to uncoated tungsten alloy (c); *pictures are in the same scale*

Worth mentioning is that the mechanism was required to be tested also in air and room temperature and some wear of the coatings was expected. For this reason, all sliding and rolling surfaces (previously coated) were additionally lubricated with Braycote 601EF. The deposition of the Braycote was done by application of the excess of Braycote on the desired surfaces and its removal with a dust-free wipe until a film of it was left. The typical method of grease plating could not be used because of assembly complexity and multiple bonding steps interchanged with the lubrication process. Often masking had to be used, especially for deposition of the coatings (MoS_2 and lead) as shown in Figure 9ab. Unfortunately, MoS_2 did tend to wear from the Hammer Lock Pins (Ti6Al4V nitrided + MoS_2) during mechanism inspection runs that were done yet before Braycote application, see Figure 9c.

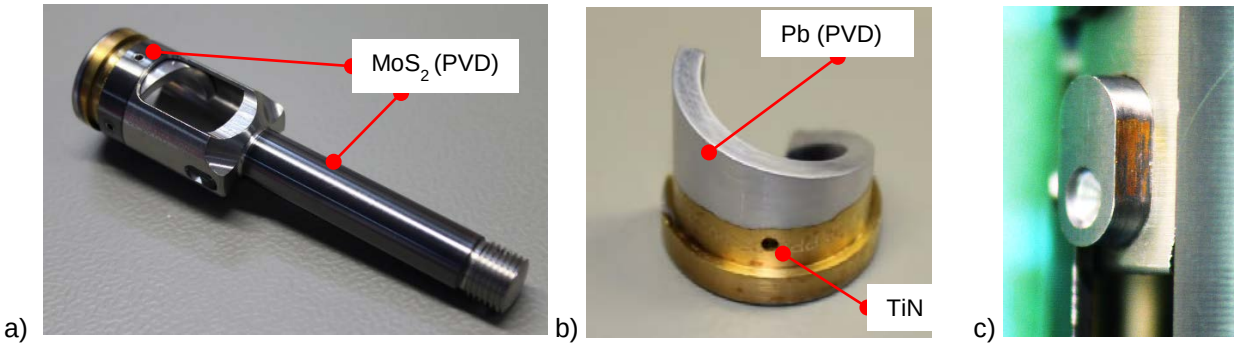

Figure 9. Appearance of different coatings and surface treatments; a) Hammer (MoS_2), b) Cam (TiN+ Pb), c) wear of MoS_2 on Hammer Lock Pin (TiN + MoS_2)

Bearings

Together with tribological coatings the bearings were implemented to take over loads induced by drive spring tensioning and cam torqueing. Angular bearings (440C, PEEK cage, O-configuration) were implemented to support rotational movement of the Roller Axis. The actual design is shown in Figure 10. The bearings are inserted on the Roller Axis part with a slip fit, they are separated from each other by the mean of the Bearing Housing where slip fit is used as well. The bearings are loaded from the side of the Motor Clutch Element, through the Outer Clutch Element that is screwed into the Roller Axis and stops on a distance washer and inner ring of one of the bearings. The washer is adjusted to the height which provides cancellation of the clearances in the bearings and stops on it after the locking torque is applied. The Outer Clutch Element has a left hand thread which corresponds to the direction of rotation of the gear shaft. This is an additional means of locking the connection (besides glue and torque applied).

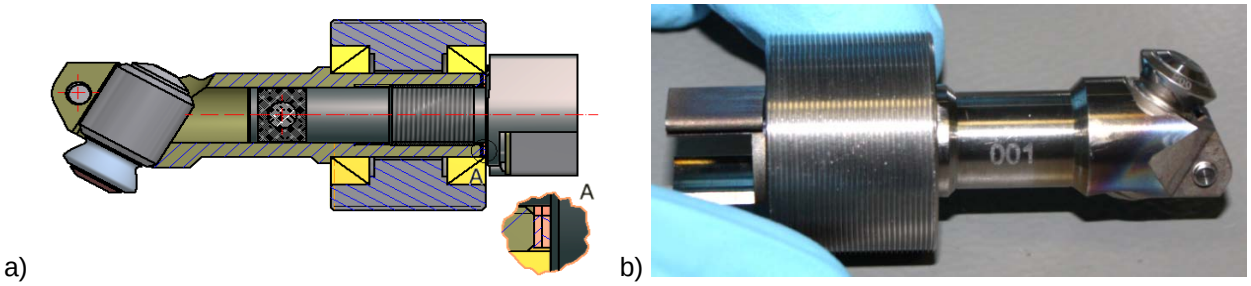

Figure 10. a) Half-section of Axis Bearing Assembly, b) Picture of Axis Bearing Assembly

The bearings are not sealed and external lubrication was applied. This is a low velocity application (15 rpm) and again the Braycote 601EF was used. As shown in Figure 11, six drops of Braycote were applied on the bearings balls with the total mass of about 0.03g (which is about 20% of the maximum volume of bearing that can be filled). Then the lubricant was spread around by rotating the bearing.

Additionally, an individual design of the bearings for the Roller Assembly was implemented (Figure 12) that significantly improved the Drive Springs loading process. To provide better load characteristics, it is

mounted on the Roller Axis at 60° angle to the main axis (see Figure 10a and Figure 12a), so not only radial but also axial forces are introduced to the assembly. As an assembly, it has 34 rotating parts (12 balls and 22 rollers), compacted into a Ø9.2x14.9 mm envelope and undergoes 87 N of radial and 50 N of axial periodic load from the Drive Springs. The design of the Roller is interesting itself and evolved a few times until it reached the presented design. It consists of the Roller Shaft which has to be a single part to ensure coaxial surface for the rotating parts. The Roller part has a press fit with Roller Shaft. The back of the Roller is closed with a Roller Washer, which does not take loads except for holding needles from escapement and it is joint to the assembly by a Roller Rivet made of 1H18N9T (EN 1.4541) stainless steel. The balls take over the axial loads. All parts, with the exception of the rivet, are 440C stainless steel hardened to 58 HRC. The interior of the Roller Assembly is lubricated with Braycote 601EF, which was applied by injection after the actual assembly – the lubricant was pressed into the Roller Assembly to fill 100% of the roller volume (which is about 0.15g). Then the Roller was rotated with 50-100 rpm for 60 seconds to remove the excess of lubricant. This resulted in 66% of lubricant remaining in the volume of the Roller (about 0.10g). The measured drag torque of the Roller with the Braycote in room temperature was c.a. 0.5 N-mm, which would have marginal influence on the gear shaft torque (close or less than 1%). One of the tests, with the pre-PFM model, revealed that even the blocked Roller can still be successfully elevated on the Cam with the provided motor, therefore increase of drag torque in lower temperatures is not critical for the mechanism. The large amount of Braycote plays an important role in sealing the Roller from unwanted debris.

a) b)

Figure 11. Angular baring lubrication: a) Braycote application area, b) close-up

a) 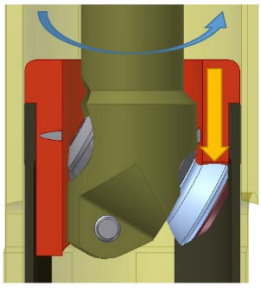 b) 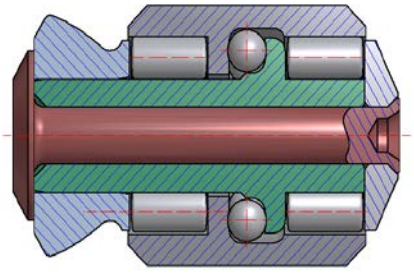 c)

Figure 12. a) Roller loading, b) Half-section of the Roller, c) Roller hold in fingers to show the scale

Launch Lock system

Functionality of the launch lock system was improved in the scope of the project. The final design allows for multiple locking and unlocking of the Hammer against the Suppressor Mass and the Suppressor Mass against the Outer Casing (i.e., Tongue Assembly) without the necessity to disassemble the whole mole mechanism (particularly important for planetary protection procedures). The Hammer Housing possesses dedicated slots (axially symmetrical on both side of the Hammer Housing) in its walls to allow for proper guidance of Hammer Lock Pins and Tongue Assembly Lock Pins and constraints the vertical movement of the traveling masses in its normal operation mode. Besides the guidance slots, it also possesses the dedicated lock notches, that are used in the locking and releasing modes of operation, see Figure 13 and Figure 14 for details.

A reverse operation of the motor is used to lock the mechanism. The motor starts to turn counter-clockwise and eventually the Roller pushes the Cam and as a result the whole Hammer Assembly. While the Hammer rotates inside the Hammer Housing, the Hammer Lock Pins encounter slope of the lock notches and slide up about 1.5 mm upwards. Eventually, they cross maximum elevation of the notch and drop into the final position in the launch lock pocket slightly loaded in that position by the Drive Springs. The motor still continues to rotate and the Hammer Lock Pins stop on the Tongue assembly fork-shaped features, see Figure 13. As a result, it is now the Suppressor Mass to start rotating in the opposite direction with respect to the Tongue Assembly. While it rotates, the cut-outs on the bottom of the Suppressor Mass change their position until the Tongue Assembly Lock Pins are positioned in the launch lock pocket of the Suppressor Mass, see Figure 14. Both pairs of the Launch Lock Pins are located in little local pockets that keep the assemblies in place during vibrations. They are not likely to freely jump out of this position because the gear shaft would have to start rotating, which requires multiple rotations of DC motor, but this is not happening during the launch.

The unlocking is just a matter of powering the motor in the operational (hammering) mode. The Roller Axis would start then to rotate clockwise and eventually the Roller encounters the Cam. The Hammer Assembly now elevates and as a result the Hammer Lock Pins are released from the launch lock pockets in the Hammer Housing. Consequently the Hammer Assembly is turned with respect to the Suppressor Mass (in the Hammer Housing) towards the normal operation guidance slots. Eventually the Hammer Lock Pins reach the opposite fork-shaped feature of the Tongue Assembly and resist against it, which allows now the Suppressor Mass assembly to start rotating backwards with respect to the Tongue Lock Pins and eventually position all the assemblies and their lock pins in corresponding guidance slots of the Hammer Housing.

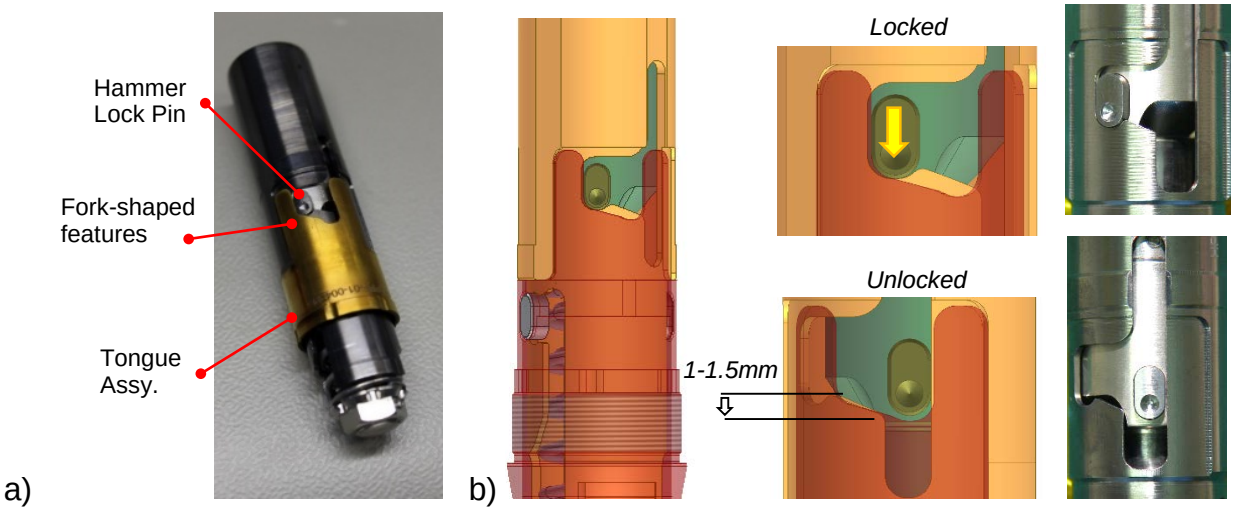

Figure 13. Launch lock design details; a) Hammer Lock Assembly with Tongue Assembly in locked position, b) Hammer locking on Suppressor Mass (right pictures without Tongue Assy.)

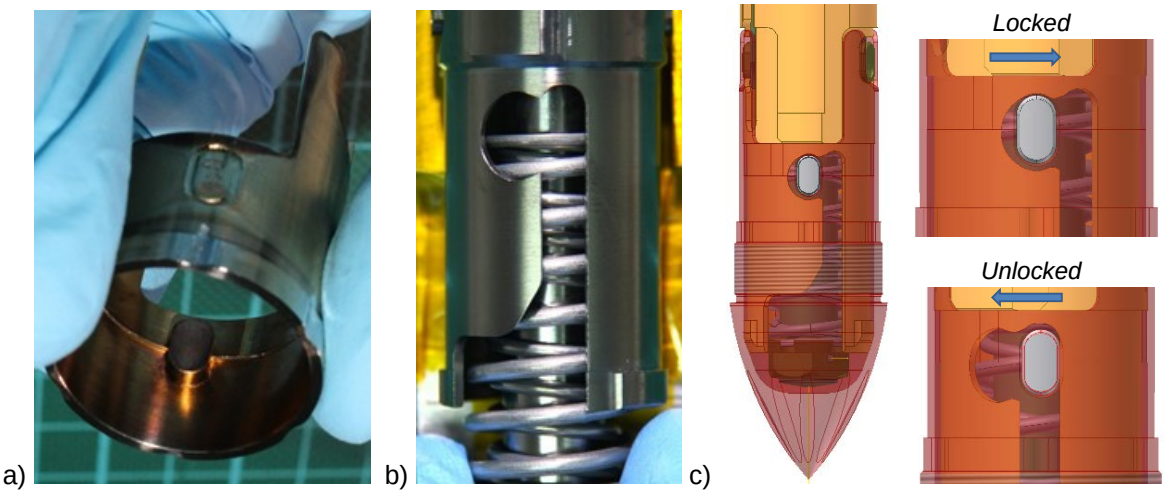

Figure 14. Launch lock design details: a) Tongue Assembly with visible one of Lock Pins, b) Hammer Housing slot for SM guidance, c) Suppressor-Mass locking on Tongue Assembly

Lessons Learned

The implemented changes allowed to achieve relatively high energy penetration strokes as for the given constraints of mass and Cam height, with much improved efficiency. The resulting average power consumption was 0.6 W (0.33/0.72 W peak values). As a result, the overall efficiency of the system is 30%. The average work cycle of the Hammering Mechanism is about 4s. Figure 15 shows the motor's current record from the first two strokes of the HM-4 unit (FM). Spring loads and release phases can be seen on this plot. When compared to the previous Figure 5, it can be clearly seen that the cam profile optimization works as expected: the uniform increase of current represents the 30° inclination slope, then the current keeps constant value (and motor constant load) until the Roller reaches the edge of the Cam.

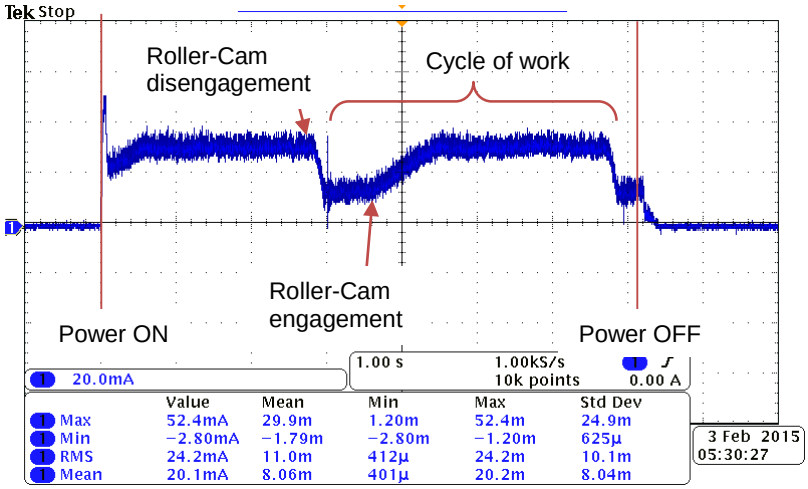

Figure 15. Current record of first two strokes of HM-4 (FM)

Besides satisfactory results that have been achieved, there were few sensitive issues encountered that are worth mentioning here.

One of such issues was connected with Tungsten alloy that was used for the Hammer and Motor Housing parts. Initially, only HE 395 alloy was used, with which CBK already had experience during development of KRET penetrator. Eventually a few cases in which this material revealed its brittle nature occurred. This happened in the Hammer parts in the area of Hammer Lock Pin location. The crack appeared in the notch

area as shown in Figure 16a and propagated. It could appear either at the moment of assembly or manufacturing. It was decided to change the material of the Hammer to HE 3925 alloy, which is more ductile. In fact the cracks in Tungsten alloy are hard to detect by direct visual inspection, also its surface features and specific reflection capabilities very often look like crack which appears not to be in the end (example shown in Figure 16b). Besides a very detailed visual inspection (microscopic with magnification over x20) of all tungsten parts, also a scanning electron microscope was used and in some cases even X-ray computer tomography (which was limited just to single millimeters of penetration due to high density of tungsten). Eddy current detection method was also investigated but due to complex shapes of the investigated parts the interpretations of measurements was not unequivocal. Starting from HM-3 model a new material was used and also all notch areas significantly modified to limit all the possible stress concentration areas. It is important to mention that no cracking was recorded for the Hammer parts during their operation and qualification tests, both for HE 395 (in HM-1 and HM-2) or HE 3925 material (for HM-3, HM-4 and HM-5).

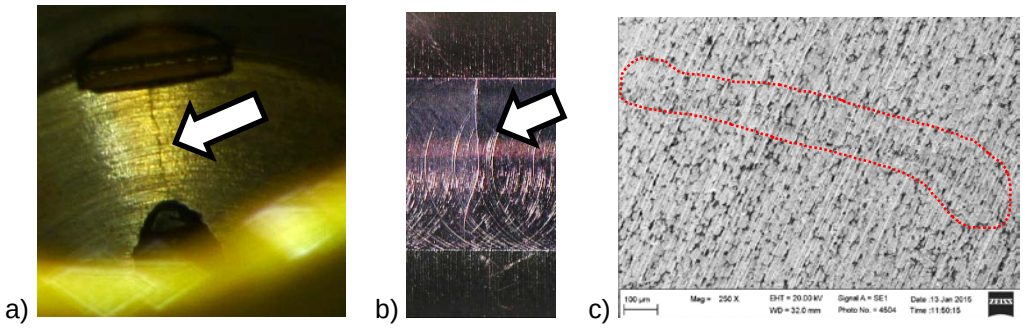

Figure 16. a) Hammer crack in the Hammer Lock Pin area (view to the interior of Hammer part), b) Motor Housing Scratch (not a crack), c) magnification of Tungsten alloy HE 3925 inspected surface (SEM, x250, inspected scratch inside the contour)

Besides tungsten alloy issues, a fatigue cracking was experienced. Models HM-1 and HM-2 have been implemented in a Clutch Spring in a form of two symmetrical 0.2-mm bands of 1.4310 steel that connected the Inner Clutch Element with the Outer Clutch Element. The purpose of the Clutch Spring was to provide the additional accumulation of energy which was used during Cam-Roller disengagement. The Clutch Spring was to kick off the Roller from the edge of the Cam and eventually reduce the losses of energy connected with rolling out. Due to the schedule constraints, the actual laboratory tests that were performed after the HM-1 and HM-2 development shown a fatigue failure of the spring after 15000 strokes (whereas qualification level was 45000 strokes). The actual effect of kicked-off rolling out can be noticed on the high-speed camera videos, but in the end the actual change of the mechanism's overall performance (stroke energy) was unnoticeable. In further models (HM-3, HM-4 and HM-5) the Clutch Spring was removed from the design. In other words, if properly designed the Clutch Spring could bring benefits to this type of the mechanism, but is not obligatory.

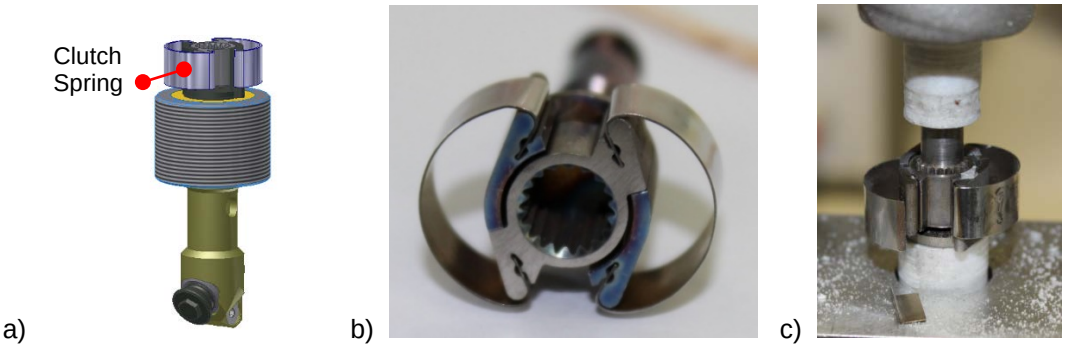

Figure 17. a) Clutch Spring location in Axis Bearing Assembly, b) The actual appearance of Clutch Spring, c) Broken Clutch Spring during the tests

The last issue worth mentioning, discovered during trial runs of the Hammering Mechanism after its integration, was its sensitivity to improper twisting of the Wire Helix with respect to the Payload Compartment and Outer Casing. The Wire Helix, which is a handcrafted component, is prone to be not fully repeatable and each mechanism required individual adjustment of the twisting angle inside the Outer Casing. The only way to do it is to properly tension it by twisting its fixation points - one with respect to the other. The direction of twisting is of a high importance and it cannot be too tight since it would interfere with Spring Support and Brake Spring and also not too wide, since it would start sliding on the Outer Casing or even block the movement of Suppressor Mass (while expanding too much while being compressed during hammering). The unpredicted influence of that tensioning was encountered during trial runs – Wire Helix when tensioned against its coil direction (in the direction that causes its diameter expanding) creates a twisting torque on the Suppressor Mass as well. This is not noticeable until the actual movement of masses begins and Suppressor Mass can undesirably slightly twist back, resulting in a situation where the fork-shaped features of the Tongue Assembly partially collide with the accelerating Hammer Assembly (namely Hammer Lock Pins). This was called a bottle-neck effect since Hammer Lock Pins for a very short time are pressed on one side by an edge of the Hammer Housing slot and corner of a fork-shaped feature in the Tongue Assembly. This cannot stop the Hammer, but can decelerate it and result in damped hammering action. The actual event sequence is shown in Figure 18a. The effect can be easily omitted when the Suppressor Mass will always be pulled by the Wire Helix in the direction indicated in Figure 18b.

a) b)

Figure 18. a) Sequence of Hammer Lock Pin movement including bottle-neck effect; b) Rear part of Suppressor Mass and Wire Helix. Arrow indicates in which direction SM should be properly pulled by Wire Helix to omit bottle-neck effect

Conclusions

The article presented the actual summary of main technological features of the Hammering Mechanism for the HP3 mole penetrator. Particularly, principle and justification for drive springs location was discussed, which should always provide stabilized pulling force on the Hammer. DC Motor operation characteristics were improved by Cam's profile optimization and confirmed with actual tests and current records. Also the principle for Cam profile design and optimization were provided with 30° initial slope inclination requirement. Significant attention was paid to the lubrication process, which was particularly important for the simplification of the design and increase of its reliability. Uncommon coatings were provided like sputtered MoS_2 on Tungsten alloy or on plasma nitrided Titanium alloy, supported by results of tribological tests. Some wear of MoS_2 on Hammer Lock Pins was experienced and additional Braycote 601EF lubrication was provided to improve the wear resistance and durability of the coatings. Besides lubrication, the bearing description was discussed including the especially interesting design of a very small Roller (Ø9.2x14.9 mm) with total of 34 rotating parts that can take over axial and radial loads. Last but not least, the novelty of the design was the Launch Lock system that allows for multiple locking and unlocking of the mechanism without necessity of penetrator's disassembly.

Problematic areas of the design were additionally highlighted. Tungsten alloy selection and its durability for high impact application was provided. Encountered problem with cracking of the material were indicated, which was solved by particularly intensive inspection process on each phase of parts development. Also

Clutch Spring design was discussed together with actual fatigue problems that led to the resignation of implementation of this mechanism's component. Eventually an assembly problem was described, connected with the bottle-neck effect on the Hammer Lock Pins movement, possible to omit by careful tensioning of the Wire Helix.

The Hammering Mechanism achieved successful performance results with power consumption kept at relatively low level, below 1 W, which proves the rightness of the implemented design.

References

1. Gromov V.V. et al.: The mobile penetrometer, a "mole" for sub-surface soil investigation. In Proc. of 7th European Space Mechanisms and Tribology Symposium. 1997.
2. Richter L. et al.: Development of the "Planetary Underground Tool" subsurface soil sampler for the Mars Express "Beagle 2" Lander. Advanced Space Research, No. 8, pp. 1225-1230. 2001.
3. Richter L., Krömer O.: Application of a Remote Controlled Hammering Drill from Space to Deep Sea. Oceans 2009 – Europe, IEEE. doi: 10.1109/OCEANSE.2009.5278132.
4. Spohn T. et al.: InSight: Measuring the Martian heat flow using the Heat Flow and Physical Properties Package (HP3). In Proc. of International Workshop on Instrumentation for Planetary Missions. 2012.
5. Lichtenheldt R., Schäfer B., Krömer O.: Hammering beneath the surface of Mars-Modeling and simulation of the impact-driven locomotion of the HP3-Mole by coupling enhanced multi-body dynamics and discrete element method. 58th Ilmenau Scientific Colloquium (IWK), Ilmenau, Germany, 2014.
6. Grygorczuk J. et al.: Technological Features in the New Mole Penetrator "Kret". In Proc. of 13th European Space Mechanisms and Tribology Symposium ESMATS, Vienna, 2009.
7. Seweryn K. et al.: Low velocity penetrators (LVP) driven by hammering action–definition of the principle of operation based on numerical models and experimental tests. Acta Astr., vol 99, pp. 303-317.
8. Stoker C. R., Gonzales A., Zavaleta J. R.: Moon/Mars Underground Mole. NASA Tech. Conf., 2006.
9. Spohn T. et al.: MUPUS–A thermal and mechanical properties probe for the Rosetta lander Philae. Space Science Reviews, (2007) 128: pp. 339–362. DOI: 10.1007/s11214-006-9081-2
10. Grygorczuk J. et al.: Advanced Mechanisms and Tribological Tests of the Hammering Sampling Device CHOMIK. In Proc. of 14th European Space Mechanisms and Tribology Symposium ESMATS, Constance, 2011.
11. Grygorczuk J. et al.: High Energy and Efficiency Penetrator-HEEP. In Proc. of 15th European Space Mechanisms and Tribology Symposium ESMATS, Noordwijk, 2013.
12. Grygorczuk J. et al.: Mole Penetrator Driven by an Electromagnetic Direct Drive (EMOLE). In Proc. of 16th European Space Mechanisms and Tribology Symposium ESMATS, Bilbao, 2015.
13. Grygorczuk J. et al.: Specialized Hybrid Rolling Bearings for Space Use – Project ROLOKOS. In Proc. of 16th European Space Mechanisms and Tribology Symposium ESMATS, Bilbao, 2015.